Systematic Search for UV-excess quasar candidates in 40 square degrees at the North Galactic Pole

Olivier Moreau, Henri Reboul

ASTRONOMY & ASTROPHYSICS
SUPPLEMENT SERIES

Astron. Astrophys. Suppl. Ser. **111,** 169-182 (1995)

Systematic search for UV-excess quasar candidates in 40 square degrees at the North Galactic Pole*,**

O. Moreau[1] and H. Reboul[2]

[1] Institut d'Astrophysique, Université de Liège, Avenue de Cointe 5, B-4000 Liège, Belgium
and CAI/DEMIRM, Observatoire de Paris, 61 avenue de l'Observatoire, F–75014 Paris, France
(European Space Agency fellow)
[2] Groupe de Recherche en Astronomie et Astrophysique du Languedoc, Université Montpellier 2,
F–34095 Montpellier Cedex 5, France

Received August 19; accepted November 29, 1994

Abstract. — We have developed a procedure (so called PAPA) for measurement of magnitudes (about 0.1 mag. accurate) and positions (with accuracy better than 0.5 arcsec) of all the objects present on photographic plates digitised with the MAMA machine. This homogeneous procedure was applied to four Schmidt plates — in U, B and twice V — covering the Palomar–Sky–Survey field PS $+30°$ 13^h00^m, a 40–square–degree zone at the North Galactic Pole. A general–interest exhaustive tricolour catalogue of 19542 star–like objects down to $V = 20.0$ has been produced and we selected 1681 quasar candidates on the basis of ultraviolet excess and, when possible, absence of any measurable proper motion. The astrometric and photometric catalogue of the candidates is given in electronic form. A first multi–object spectroscopy of a few candidates confirms validity of the selection.

Key words: quasars: general — surveys — techniques: photometric — astrometry — stars: population II — white dwarfs

1. Introduction

Thanks to their striking intrinsic luminosity, quasars may be considered as landmarks of the far Universe. Though the local distribution of luminous matter has nowadays been fairly well determined by the study of the space distribution of galaxies (see, e.g., de Lapparent et al. 1988), we know very few about the structuring evolution between the scale of superclusters and that of the very weak density fluctuations recently derived from the observations of the cosmic microwave background with satellite COBE (Smoot et al. 1992) and the Tenerife instruments (Hancock et al. 1994). A better knowledge of the space distribution of quasars, seen as markers of possible very large scale structures (VLSS), might give some hints about that question. However, these objects are rather rare: their surface density is about 25 per square degree down to a limiting B magnitude of 20.0 (Koo & Kron 1982) and moreover the angle covered by these possible VLSS should be very wide: at redshift 1.5, a structure with a present time comoving extension of 1 Gpc would cover a solid angle of about 100 square degrees in the sky (see Reboul 1988). So, progress in that way can only be done by collecting large and homogeneous samples of quasars.

On the other hand, the discovery of a larger number of quasars may be a source of new gravitational mirages and/or cases of binary quasars, both types of objects presenting a high cosmological interest (see e.g. Surdej & Refsdal 1992 and Reboul et al. 1986). Moreover, quasars represent useful background light sources allowing the exploration of the intervening intergalactic and galactic medium as well as they are distant reference objects helpful for high accuracy astrometry. More generally, in order to get a better understanding of the physics and evolution of quasars, it is desirable to increase the number of known objects.

However, quasars are characterized by their spectrum and, even using a multi–object spectrograph, a systematic spectrography of every object down to $B \simeq 20$ in wide regions of the sky would be far too much telescope–time consuming. A selection of quasar candidates in wide fields is thus necessary, in order to strongly reduce the number of objects to observe by spectroscopy. With this aim,

Send offprint requests to: O. Moreau *(Paris address)*
*Based on photographic plates obtained with the Palomar 48 inches and OCA 0.9 m Schmidt telescopes, digitisations made with the MAMA measuring machine of C.A.I. (I.N.S.U., Paris) and observations obtained with the CFH 3.6 m telescope
**Tables 7, 8 and the quasar-candidate catalogue are available electronically at the CDS via ftp 130.79.128.5

numerous programmes for quasar–candidate optical selection have been undertaken world–wide these last years (see, for a review, Foltz & Osmer 1988; Moreau 1992b). The availability of accurate and high–speed microdensitometers such as APM (Kibblewhite et al. 1984), APS (Pennington et al. 1992), COSMOS (Mac Gillivray & Stobie 1984) or MAMA (see Sect. 3) has allowed automatic (and then expected to be objective and homogeneous) exhaustive measurements of large photographic documents like Schmidt plates, an activity formerly reserved to visual analysis. So, it is possible, among many applications, to operate an accurate and homogeneous wide-fielded selection of quasar candidates from direct photographic plates as being performed in the southern hemisphere, for example, by Irwin et al. (1991) and Warren et al. (1991) using APM and Stobie et al. (1987, 1992), Cristiani et al. (1991) and Goldschmidt et al. (1991) with COSMOS.

For all the purposes above mentioned, we intend to perform a homogeneous, wide (300 square degrees) and deep (down to magnitude $V \simeq 20$) survey of the North Galactic Pole (NGP) with a special attention to a systematic search for quasar candidates (Moreau 1992a). The conjunction of such wideness and depth is not common among the on–going projects and this region at the NGP has not yet been systematically searched for quasars in wide fields. We have developed an automatic procedure of total reduction (cataloguing) of Schmidt fields for multi–colour surveys permitting, among other applications, the selection of quasar candidates and we have choosen to display in this paper both the detail of the reduction method and the list of UV–excess candidates that we have systematically selected in a first 40–square–degree field at the NGP.

2. The observational material

The main part of the observational material we used consists of three original photographic plates in U, B and V passbands respectively, taken in 1962 with the Palomar 48–inch Schmidt telescope. In fact, a considerable photographic plate material has been taken there by J. Berger, in the frame of a visual search for faint blue stars in Palomar–Sky–Survey (PSS) fields at high galactic latitudes (Berger & Fringant 1977). So, the present field (area: 40 square degrees; centre: α_{2000} = 13 h 06 min 56 s, δ_{2000} = +29° 13′ 24″), almost centred on the selected area SA57, belongs to a set of eight ones covering a 300–square–degree contiguous zone around the NGP. We also obtained in 1990 from the 0.9 m Schmidt telescope of Observatoire de la Côte d'Azur (OCA, France) a V plate covering an area of 27 square degrees and centred on position α_{2000} = 13 h 08 min 38 s, δ_{2000} = +29° 22′ 00″; in fact, that plate was only used for astrometric measurements in this work. Table 1 summarizes the observational characteristics of the four plates presently studied. The Palomar B plate was sent to us with a small missing broken corner (about 5 cm^2 lost i.e. 0.2 square degrees in the sky). Due to a strong hypersensitivity at its edge and to the presence of calibration density steps, the fairly usable field of the OCA plate is restricted to 22 square degrees.

Table 1. Palomar (PS) and OCA plates used

Plate N°	exposure	emulsion	filter	colour	epoch
PS 6557	15 min	103aD	#3	V	1962.321
PS 6559	60 min	103aO	UG1	U	1962.321
PS 6560	7 min	103aO	GG13	B	1962.321
OCA 2465	90 min	IIaD	GG495	V	1990.247

3. The digitising machine

The huge amount of data present on 35 cm × 35 cm Schmidt plates such as Palomar ones imposes the use of a measuring machine if one aims at an homogeneous and quite exhaustive extraction of the recorded information. We used MAMA (*Machine Automatique à Mesurer pour l'Astronomie*), the high–speed and high–accuracy multichannel microdensitometer of Centre d'Analyse des Images (C.A.I.) located at Observatoire de Paris (see Guibert & Moreau 1991 for a presentation of MAMA and C.A.I.; Moreau 1992b for some technical data about the scanning system). Systematic scans of the plates have been performed, with a pixel size of 10 μm (corresponding to about 0.65 arcsec on the plates) and a 4096–grey–level quantification. Note that before the scan of each plate, the MAMA detector was systematically calibrated on a small area of the plate by gain and dark current measurements for each of the 1024 photodiods.

4. PAPA method, inventory of objects on plates

In a former paper (Berger et al. 1991) devoted to the study of 1221 UV–excess objects and hereafter labelled B91, we have presented a method for the measurement of object magnitudes and celestial positions on Schmidt plates digitised with MAMA. Nevertheless, B91 work dealt with previously listed objects, randomly accessed using the so–called *pavés* digitising mode of MAMA. Here, we are going ahead with the systematic measurement of all the objects that can be detected on the photographic plates analysed. The PAPA procedure (*Programme Automatique de Photométrie et d'Astrométrie*) consists in the full photometric and astrometric reduction of digitised plates by calibration using standard stars. Applied respectively to each of the four plates quoted in Sect. 2, it led to four exhaustive catalogues including magnitudes (OCA one excepted) and (α, δ) coordinates of every star–like object detected.

4.1. *Digitising the standard stars*

For each plate, in order to make easier the requisite identification of the astrometric and photometric standard stars, we digitised 128×128–pixel images (corresponding to 86 arcsec × 86 arcsec in the sky) around the positions of each of them. For this operation, MAMA was used in its *pavés* acquisition mode (see B91); let us recall that in this accessing mode, the transformation of (α, δ) coordinates of the objects into (x, y) table positioning and scanning orders is obtained by an adjusting program using acquisition, visualization and pointing of at least 20 bright stars. 260 standard stars were digitised (41 photometric and 219 astrometric, somewhat less on OCA plate); this required a 1–hour machine run (including automatic focussing and object detection described below) for each plate.

4.2. *Full–plate acquisition*

The second step of the scanning sequence was the complete digitisation of the plates. About 1.2 10^9 pixels were acquired from each of the three Palomar plates in 14–hour runs also including focussing and object detection. The OCA plate is smaller: 9 hours were sufficient for the analysis of 0.8 10^9 pixels from it. Note that a thin margin of the plates was obscured by a mylar frame placed between them and the MAMA table glass. This anti–Newton device caused the loss of some marginal objects: free field was limited to 34 cm × 34 cm for Palomar plates.

4.3. *Sky background determination and object detection*

An automated detection of objects was performed by segmentation of the images (either from *pavés* or full–plate modes) at a fixed density value above the local sky background; we considered as an object every domain of more than 9 connected pixels whose density is above the threshold (see Slezak et al. 1988). No smoothing of the images was operated.

The local values of the sky background were computed in subimages of 128×128 pixels. So, one unique sky background value was affected to every standard–star *pavé* and, for the reduction of full–plate measurements, the whole plate was squared by a mesh of 128×128–pixel cells in which the sky background is considered as constant. The determination of the local sky backgound value is based on the density histograms of the pixels of a given cell. A raw kappa–sigma clipping is applied to the histograms so that 160 density levels only on both sides of their maxima are taken into account. The most probable value of the sky value is then computed using the method described in B91 which is based on the modelization of the remaining part of the histograms (Bijaoui 1980). The standard deviation from it of the sky background values at each pixel is also calculated in each cell. In order to estimate on each plate the mean value of this "pixel–to–pixel" standard deviation, σ_{px}, we examined a 1024×1024-pixel zone and averaged that of the 64 cells determined therein. This operation was conducted before the acquisition run because it was necessary to know σ_{px} for the choice of segmentation thresholds. Table 2 gives the value of σ_{px} for each plate we analysed.

Variations of background values all over the plates represent a real problem for photometry. As a matter of fact, one has to remark that the background we compute is in fact a combination of the response of the emulsion to the pure astronomical sky background and of its base–plus–fog density. As well, what we call background variations may also be due to geographical inhomogeneities of emulsion sensitivity and not only to actual variations of the sky background. In order to examine these variations, we have plotted in Fig. 1 the local background value at every position where an object was detected on each plate that we photometrically reduced in Sect. 4.4, i.e. the three Palomar ones. Values are given in MAMA photographic densities, which are not diffuse densities. The spikes that can be observed in the different plots of Fig. 1 are due to five very bright stars, the five brightest ones of the field (data about them are in Table 3) which pollute the local background and then locally cause a set of sprrious detections due to noise and not to real objects. As a matter of fact, we have done statistics on the value plotted in Fig. 1 in order to quantify the geographical variation of the background value all over the plates. Mean value and "cell–to–cell" standard deviation from it, σ_{ce}, are displayed in Table 2; data for OCA plate come from local background measurements at the position of the 1221 objects of B91, which are well spread all over the plate (this work was done in the frame of a variability study of these particular objects, see Moreau 1992b). Apart from the quoted spikes, one can see that the background values are quite homogeneous all over the Palomar plates (standard deviation on V plate is enhanced by the strong spikes due to bright stars) and thus a reliable photometry should be achieved on them within the whole field.

Table 2. Background parameters of the different plates, in MAMA photographic densities

Plate N°	colour	σ_{px}	mean on plate	σ_{ce}
PS 6557	V	0.067	0.338	0.051
PS 6559	U	0.067	0.288	0.022
PS 6560	B	0.068	0.300	0.027
OCA 2465	V	0.077	0.536	0.081

In order to get rid of the false detections due to background pollution, we rejected from the catalogues all objects with a local background value departing from the plate mean of more than 5 times the standard deviation σ_{ce} of these values. Objects with departure larger than 3 times this standard deviation were flagged in the cata-

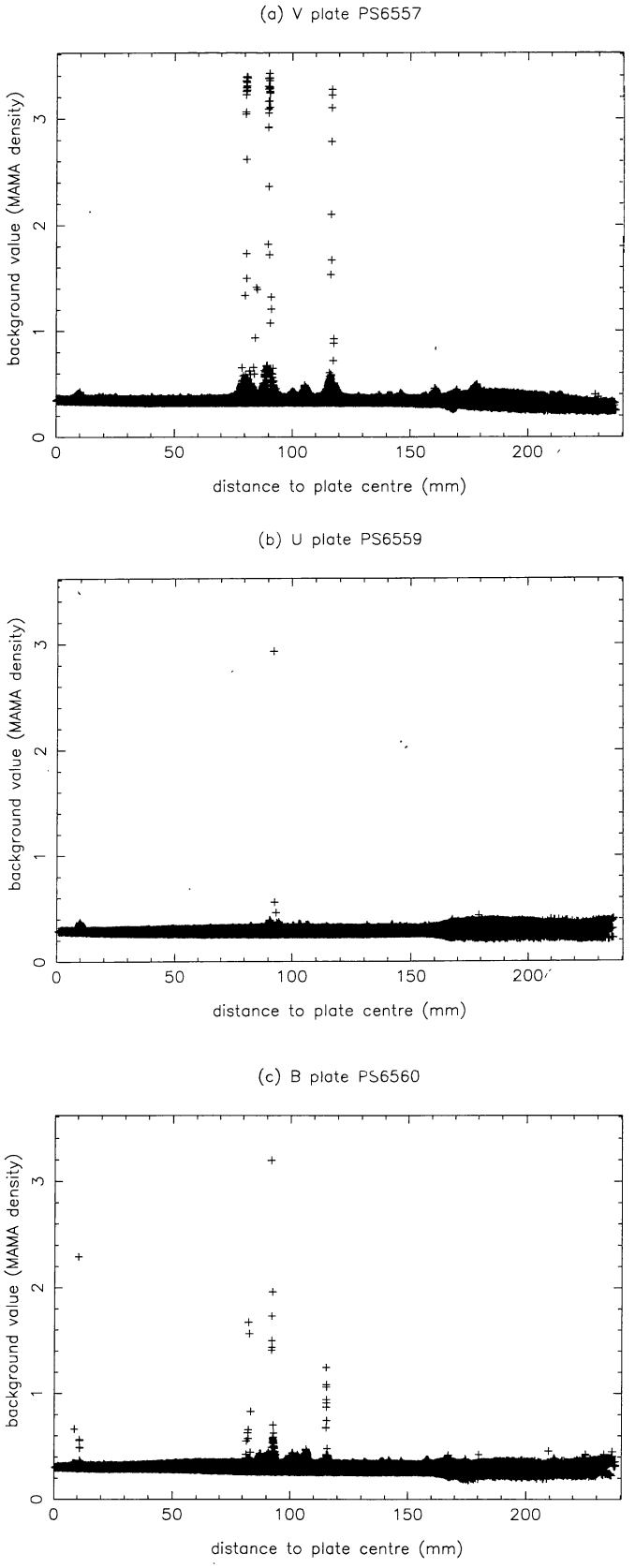

Fig. 1. Local background (in MAMA densities) on Palomar plates as a function of object distance from plate centres

Table 3. Very bright stars of the field which pollute the local background; V magnitudes are from the Bright Star Catalogue (Hoffleit & Jaschek 1982)

Star name	distance to V plate centre	V magnitude
HD 113865	10 mm	6.54
41 Com	81 mm	4.80
HD 114092	85 mm	6.19
β Com	90 mm	4.26
37 Com	117 mm	4.90

logues because this may indicate an error in the magnitude measurement of the object.

The threshold for segmentation of images was set to 2.3 times σ_{px} above the local background. This adopted value is a compromise between misses of objects present above the limiting magnitude of the plates if it is chosen too high and detections of spurious (due to noise) objects if set too low. This part of the procedure supplied in fact two catalogues for each plate, a first catalogue of objects detected inside the *pavés* of standard stars and an exhaustive one containing all those detected in the whole scanned area. Main file entries are (x, y) machine coordinates of the objects, area (number of pixels inside the segmented contour), density flux (sum of the density values of pixels), local background value and morphological parameters including ellipse axis parameters of the contour. It is to note that in order to clean the catalogues from plate scratches, we temporarily (see Sect. 4.6) rejected the objects presenting a ratio larger than 3 between their ellipse major and minor axes. The astrometric and photometric standard stars were visually identified in the *pavés* so that they were easily picked up in the first catalogue.

4.4. *Photometric reduction*

The photometry of objects is done through a log(flux)/magnitude calibration curve obtained from a fit between the points given by the photoelectric standard stars measured in the *pavés*. In fact, only the three Palomar plates were photometrically reduced. Since they present no calibration step, the photometric calibration of the plates was performed using photographic density flux measurements. Consequently, systematic effects due to the non–linearity of the photographic emulsion response combined with local variations of the sky background and of the plate sensitivity may appear; we tried to quantify these effects in B91, which concerns the same plates, and did not find any significative trend (we have seen in Sect. 4.3 that the plates show a quite uniform background). Moreover, it is to note that the photometric standards available in SA57 are numerous and well distributed in magnitude and that we are, in this work, mainly interested in star–like objects which

are less affected than extended sources by non–linearity effects.

We used the calibration sequence described in B91, obtained by merging two purely photoelectric ones, from Purgathofer (1969) and Baum (1960) respectively. Let us remind that we eliminated from these sequences the reddest objects (because we mainly aim at measurements of UV–excess objects) and the brightest ones that are saturated and out of the magnitude range we are interested in. Moreover, a few of these calibration stars — too faint — were not detected in U and B. In fact, we used exactly the same photometric standards that in B91. Polynomial fits of the relation between the standard magnitudes used and the decimal logarithms of MAMA density fluxes are shown in Fig. 2. Polynomial degrees were set to 4 for the B plate and to 5 for the two other ones. Residuals on calibration (standard deviation of the magnitude difference between that of standard stars and the fitted curve) are displayed in Table 4, they lie around 0.07 mag. This gives an estimate of the photometric accuracy achieved but it is to note that the photoelectric standards we used are concentrated at the centre of the field. So, errors may be larger at the edges of the plates. Globally, we believe that our magnitude measurements are subject to a standard deviation of about 0.1 mag but such an accuracy is obviously not achieved at the faint end of the calibration curves and ones has to be cautious with measurements lying within say 0.5 mag. above the calibration limit. As can be seen in Fig. 2, we essentially restricted the validity of the fitted relations to the flux range covered by the photometric standards. The magnitude ranges of our photometric calibrations are also shown in Table 4 together with the number of detected objects effectively calibrated.

Table 4. Photometric calibration

Plate N°	colour	mag. range	residual	nb. of objects
PS 6557	V	9.42 – 20.32	0.07 mag.	126948
PS 6559	U	9.90 – 19.59	0.06 mag.	32336
PS 6560	B	9.78 – 19.31	0.08 mag.	30683

Finally, we plotted in Fig. 3 the magnitude histograms obtained from the exhaustive photometric reduction of the three Palomar plates. These histograms do not show any flagrant incompleteness in our catalogues down to the faint ends of the calibration ranges (i.e. 19.6 in U, 19.3 in B and 20.3 in V), at least for stellar objects. As a matter of fact, at this stage, the catalogues contain both star–like and diffuse objects.

4.5. *Astrometric reduction*

The astrometric reduction is done using proper–motion–corrected positions of reference stars from the PPM star

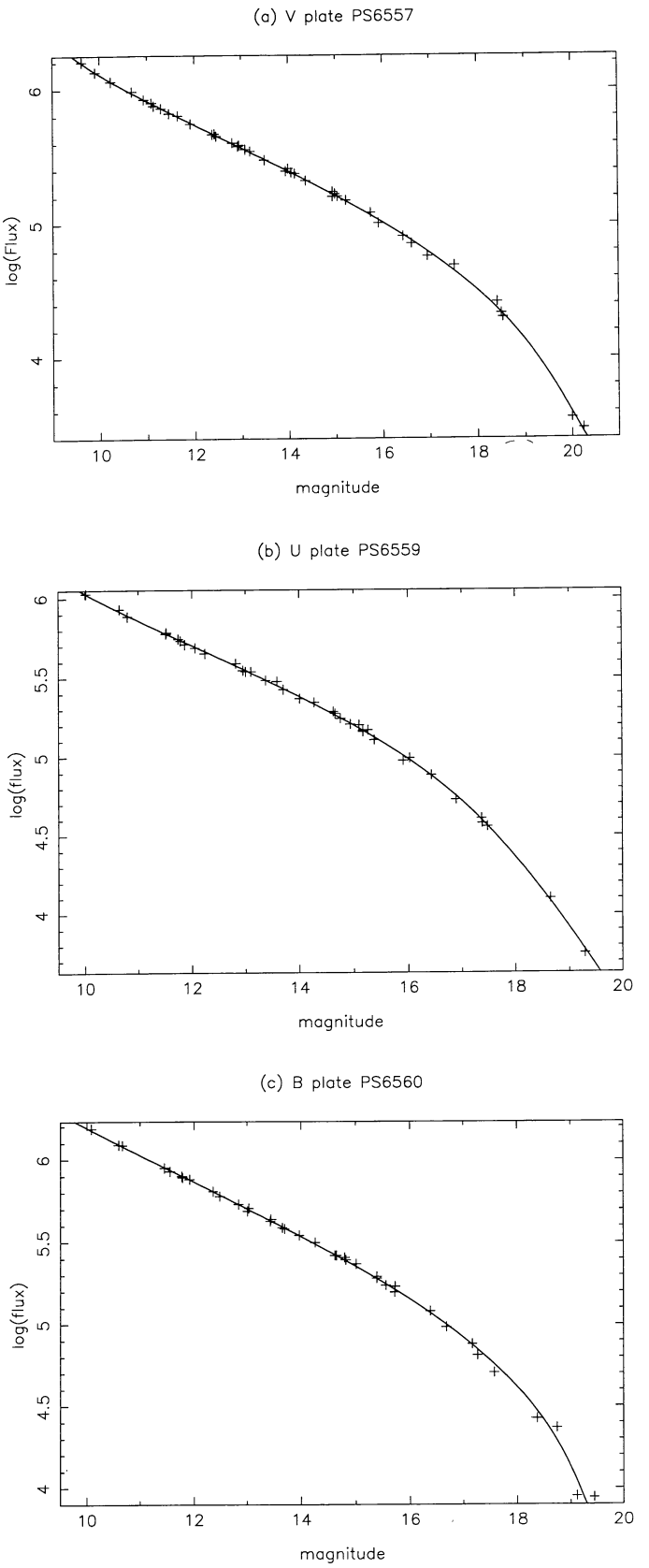

Fig. 2. Photometric calibration curves for the Palomar plates

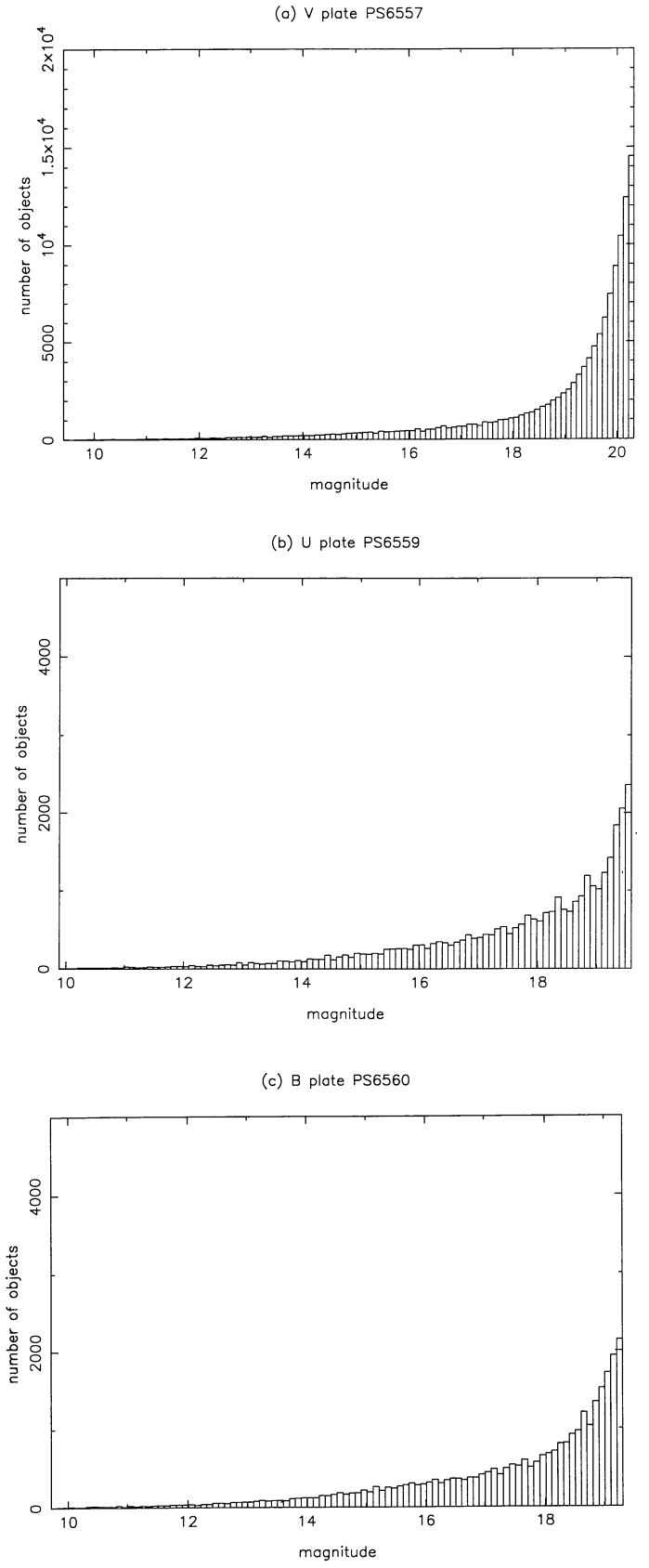

Fig. 3. Magnitude histograms after photometric calibration of the three Palomar plates respectively in V, U and B passbands (bin size is 0.1 mag.)

catalogue (Röser & Bastian 1991): the Schmidt plates are modelized by a third order bidimensional polynomial fitting in order to perform a transformation from (x, y) plate coordinates to (α, δ) celestial coordinates. Such a third–order modelization is mandatory for astrometric reduction of Schmidt plates because of the deformation they suffer in the telescope when matched to the Schmidt focus surface and because of the wide field they cover.

The standards were selected among the 219 PPM stars present in the 40–square–degree field. Some of these stars were lost due to the mylar frame (see Sect. 4.2), some were rejected — being double, too bright or affected by plate defects — after visualisation of the digitised images of the *pavés*; about 150 reference stars then remained for the different Palomar plates and 87 for the OCA one, whose restricted field is quite smaller. These stars were submitted to the fitting program, that provides an iterative rejection of standards whose residual is larger than 2.7σ; the number of standard stars effectively used after rejection by the model of each plate is displayed in Table 5. We have checked that the fields are fairly well geographically covered by PPM stars, this is mandatory for a good modelization of the plates. Mean residuals on the transformation $(x, y \longleftrightarrow \alpha_{2000}, \delta_{2000})$ are also summarized in Table 5. Their values lie around 0.3 arcsec, giving an estimate of the astrometric accuracy performed; however, it is presumable that the effective accuracy is lower at the extreme limits of the plates.

Table 5. Astrometric calibration

Plate N°	colour	nb. of stars used	residual
PS 6557	V	142	0.31"
PS 6559	U	158	0.29"
PS 6560	B	151	0.29"
OCA 2465	V	85	0.37"

Globally, the accuracy on our object positions should be better than 0.5 arcsec. It is to note that the residuals observed on standard stars are mainly due to the PPM catalogue (which is the best available at the time of this reduction) and are not imputable to MAMA measuring errors. Indeed, MAMA absolute positional accuracy is about 1 μm, i.e. 0.07 arcsec on the plates (Soubiran 1992).

4.6. *Diffuse object separation*

The reduction techniques we used, particularly for photometry, are especially suited to star–like objects, i.e. objects whose images on plates are unresolved. Moreover, as we aim at quasar–candidate selection, it was necessary to remove the diffuse objects from the catalogue, we mean those whose image is resolved i.e. different from the point–spread function of the measurement chain. The separation of diffuse objects from stellar ones was mainly performed

using area and flux parameters from the catalogue of objects from V_{1962} plate (PS6557), which is the deepest one. We used for that purpose a classical log(area)/log(flux) diagram displayed in Fig. 4. A thin sequence appears in this plot which is the locus of star–like sources. Objects whose area is excessive in regard to their flux depart from this sequence: as we are observing at high (polar) galactic latitude, they mainly should be galaxies. The stellar sequence was fitted by a fifth–order polynomial with a 2.0σ iterative point rejection among the objects having an area larger than 40 pixels. A frontier between star–like and diffuse objects was then interactively plotted at 0.115 log(flux) units below the fitted polynomial. However, when the flux is too low, stars and galaxies merge in the diagram and the separation becomes quite impossible so we restricted the area range of our discrimination to objects having more than 65 pixels. This restriction is represented in the plot by a vertical line. 4782 objects out of 126948 were classified as diffuse using that diagram and then removed from the V_{1962} catalogue hereafter used. They nevertheless constitute a catalogue of highly–probable galaxy candidates with rather accurate (α, δ) positions, and V magnitudes that we consider as tentative because our magnitude measurement method is not suited to extended sources. Magnitude histogram of these objects is however plotted in Fig. 5, it shows that completeness of our galaxy–candidate catalogue is limited to about $V = 18.2$ because of the minimal area we imposed for the separation.

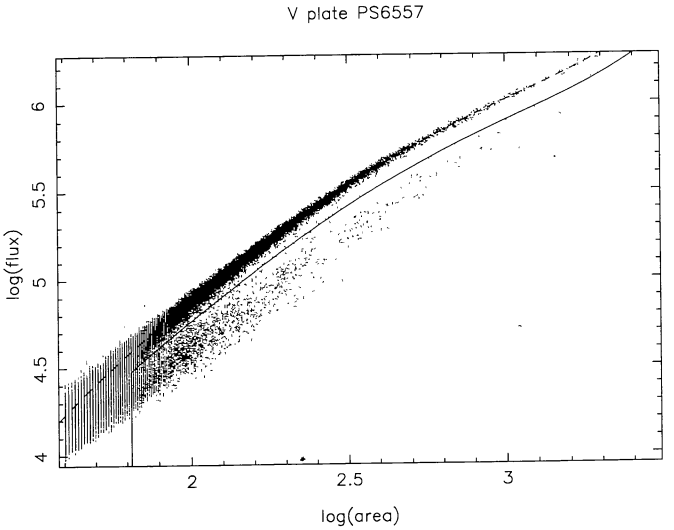

Fig. 4. Diffuse–object separation

Note that we appended to the diffuse–object catalogue 35 objects that were formerly rejected for excessive oblateness (Sect. 4.3) on more than one of the three Palomar plates. We thus intend to evacuate plate scratches and asteroid trails without losing genuine very elongated objects. Indeed, such unusual sources may be more effectively

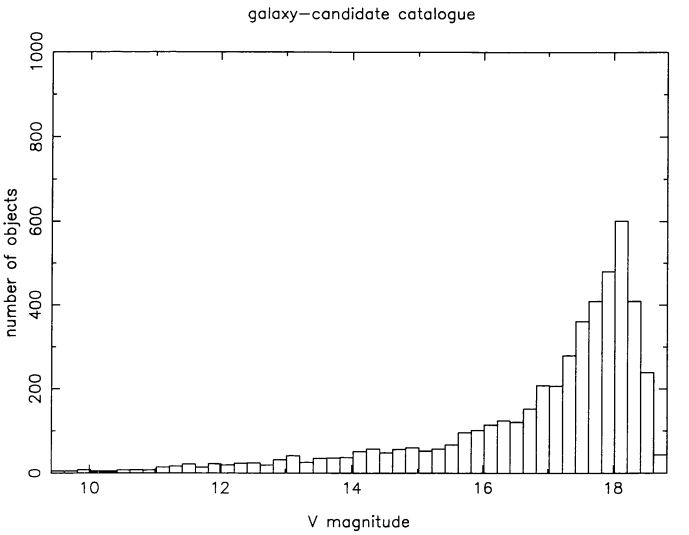

Fig. 5. V magnitude histogram for objects selected as diffuse with the log(aire)/log(flux) criterion (bins of 0.2 mag)

picked out that way than by the log(aire)/log(flux) criterion.

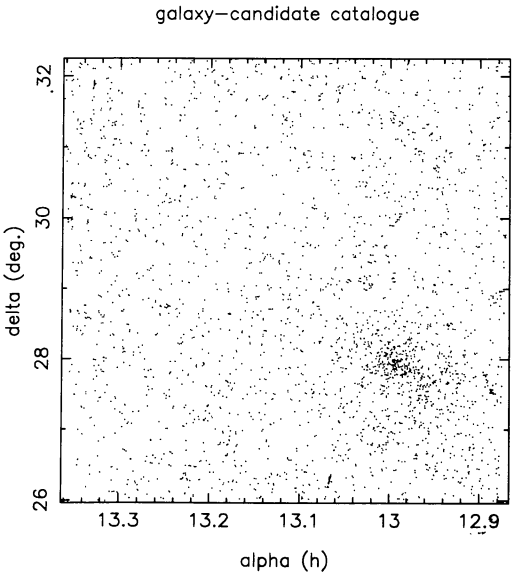

Fig. 6. Surface distribution of the galaxy–like objects catalogued

The final catalogue of 4817 galaxy candidates might be useful for other investigations. We plotted in Fig. 6 the bidimensional distribution of these objects, their mean surface density is 120 per square degree. One can still recognize the Coma cluster at $\alpha \simeq 13$h and $\delta \simeq +28°$ despite the background of remote galaxies. We also note that some bidimensional structures may exist.

4.7. *Cataloguing*

Cross–identification of star–like objects between the catalogues obtained from analysis of the three Palomar plates allowed the production of a tricolour UBV catalogue. In practice, we paired together V_{1962} and U_{1962} catalogues and then V_{1962} and B_{1962} catalogues and searched for objects common to both associations. Objects were recognized from one plate to another by their (α, δ) coordinates; histograms of position discrepancies between catalogues are displayed in Fig. 7. As the plates were taken during the same night, no proper motion will appear so the maximum discrepancy admitted for object association was 2.0 arcsec, this threshold taking into account the astrometric accuracy expected to be achieved after Sect. 4.5 and Fig. 7. We obtained a catalogue of 19542 star–like objects with (α, δ) and V magnitudes from the V_{1962} plate, $U-B$ and $B-V$ colour indices and complementary data such as position discrepancies between the different plates, morphological parameters, a log(aire)/log(flux) parameter and, for some objects, the local–background flag defined in Sect. 4.3.

Magnitude histograms of objects from this UBV catalogue are shown in Fig. 8; its completeness seems to be limited to about 18.2 in U and B and even 16.8 in V by the effect of the pairing between the three plates. Indeed, if the three limiting magnitudes are — and were intended to be — well suited to the measurement of UV–excess objects, the U and B plates actually are not deep enough compared to the V plate for the general — and much redder — sky population: it is well known that the bulk of sources have positive $U-V$ and $B-V$ as evident in Fig. 9, where is displayed the colour–colour diagram of the UBV catalogue. But the upper left part of this diagram clearly shows the widely spread population of UV–excess objects we aim at, well distinct from the characteristic point cluster essentially due to main–sequence stars (halo and disk mixed populations). A line of equation $U-V$=0.1 provides a fair border in the diagram between the two populations of objects. It is worthwhile to note that the present study must be quite exempt of colour blurring due to intrinsic variability of objects since the U, B and V 1962 plates have been obtained during the same night. In particular, our colour measurements are free from effects due to quasar or AGN variability, this is a characteristic not so common among the recent multi–colour–selected quasar surveys (as pointed out by Hewett & Foltz 1994).

Both the galaxy catalogue and the exhaustive multi–colour catalogue of star–like objects do constitute multi–purpose homogeneous data sets. Some applications could be star counts at high galactic latitude in comparison with stellar population models, correlation with catalogues obtained from space in other wavelength ranges towards the caracterisation of extragalactic sources, etc.

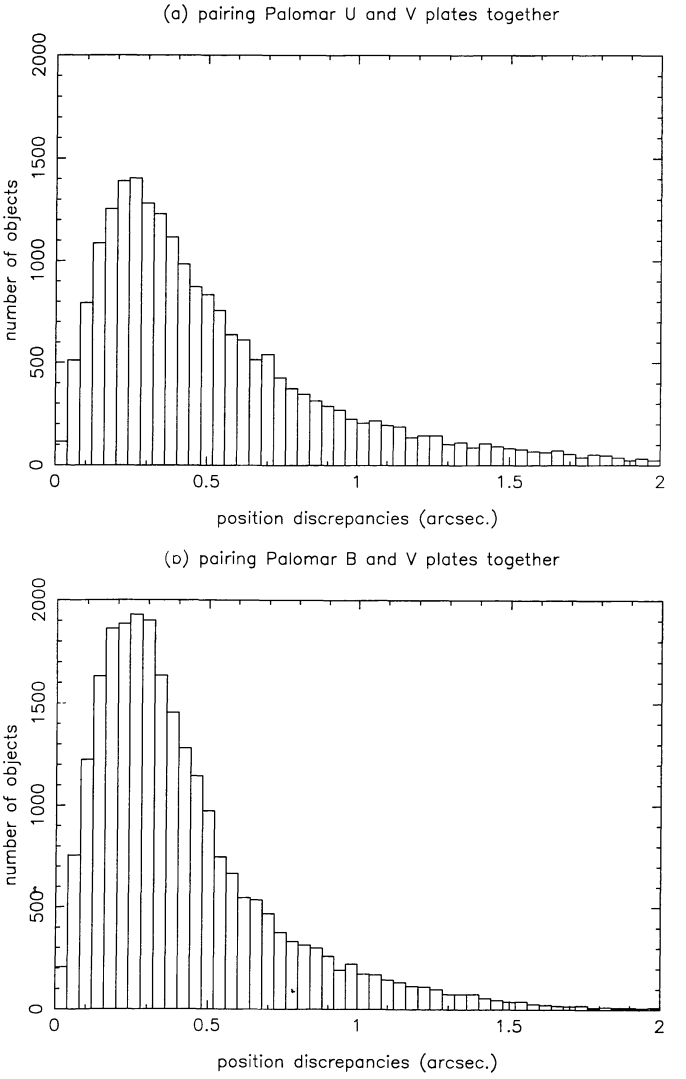

Fig. 7. Position discrepancies between catalogues a) U versus V_{1962} (20595 objects), b) B versus V_{1962} (24352 objects); bin size is 0.04 arcsec

5. Quasar–candidate selection

5.1. *Colour*

It is well known that low redshift quasars, with $z \lesssim 2.2$, show an ultraviolet excess. Practically, a selection of low–redshift quasar candidates can be done among catalogues of star–like objects with a colour criterion based on $U-V \lesssim 0$ — as already used by Berger & Fringant (1977) and corresponding to tables II, III and IV of Haro & Luyten (1962) —, say for example $U-V < 0.1$ (see Moreau 1992b). In this part of a $U-B/B-V$ diagram, giants and main–sequence stars of spectral type B0 to A0 belonging to the galactic disc do not interfere with the candidate selection because they are very bright objects. Indeed, at such polar galactic latitudes, the disc extends to a maximum of 2 kpc and all the stars of this kind have an abso-

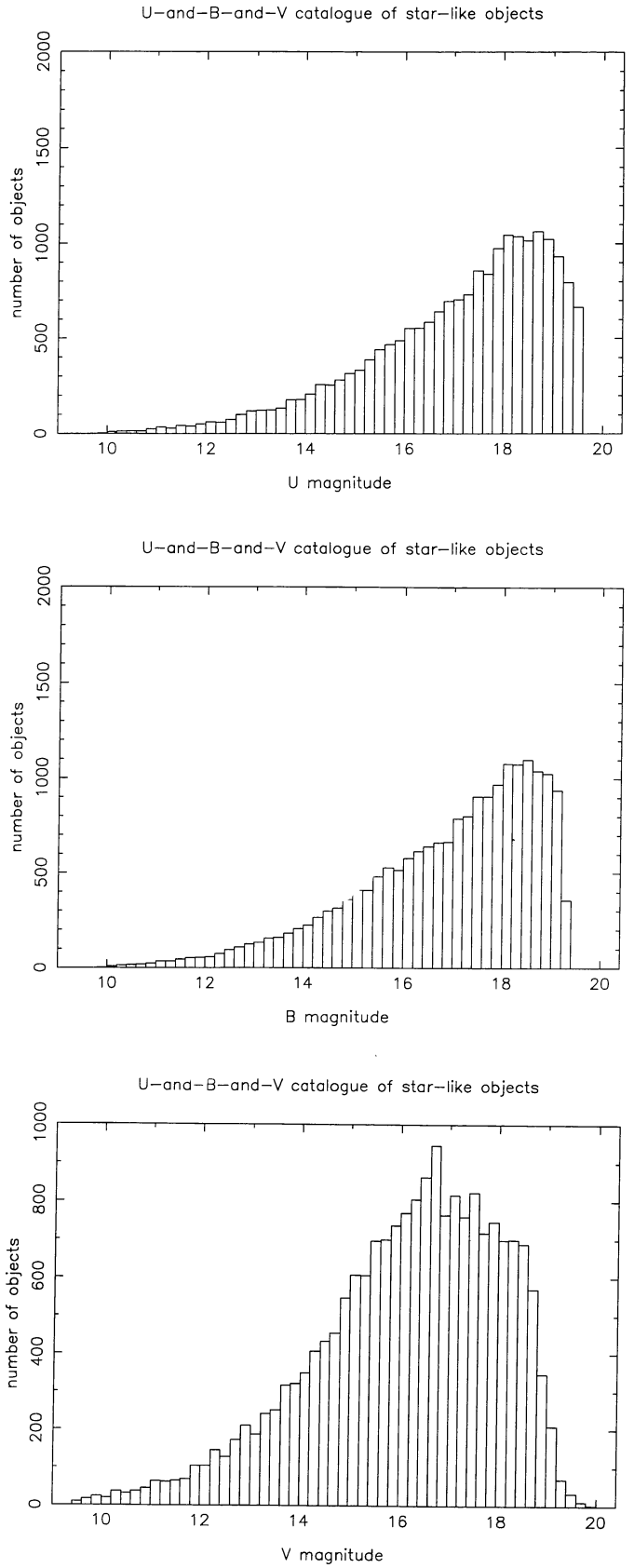

Fig. 8. Magnitude histograms of objects of the multicolour catalogue (1 bin for 0.2 mag)

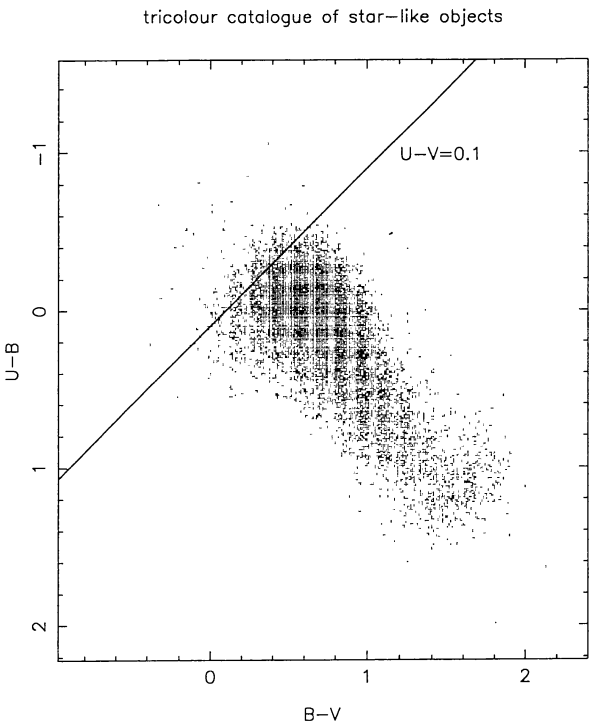

Fig. 9. UBV colour diagram of the catalogued star–like objects; the line $U-V=0.1$ has been plotted

lute magnitude smaller than 1.5 (Allen 1973) so, they will appear with a visual magnitude brighter than 13. As well, halo stars of such spectral types have already left the main sequence (the halo main sequence turn–off is believed to occur at $B-V \simeq 0.4$) and occupy therefore other parts of the colour diagram, except for horizontal-branch stars. On the contrary, with such a colour criterion, it is well known that hot white dwarfs will pollute the quasar–candidate catalogue. But quasars do not show any proper motion, so candidates for which a proper motion is observed may be removed from the list and this provides a rather efficient way to clean the candidate catalogue from some white dwarfs (Moreau 1992b). At last, above $z \simeq 2.1$, the $U-B$ colour indices of quasars rapidly increase for two reasons: the strong Lyα emission line enters the B passband and the part of the quasar spectra most depleted by the Lyα forest absorption enters the U one.

Taking into account these theoretical considerations, the accuracy of our photometric measurements ($\simeq$ 0.1 mag.) and referring to the effective colour diagram of the objects we measured (Fig. 9), we selected as quasar candidates 1759 objects having $U-V<0.1$, among the 20595 star–like objects paired from U and V plates (Sect. 4.7). The completeness of the pairing is limited by the U plate, i.e. at its calibration limit U=19.6; for objects having $U-V<0.1$, it corresponds to a limit of $V \simeq 19.5$, as confirmed in Fig. 12 which displays 19.4 as a probable completeness limit of the candidate catalogue. The mean

surface density of the candidates is 44 per square degree. Their bidimensional distribution is displayed in Fig. 10.

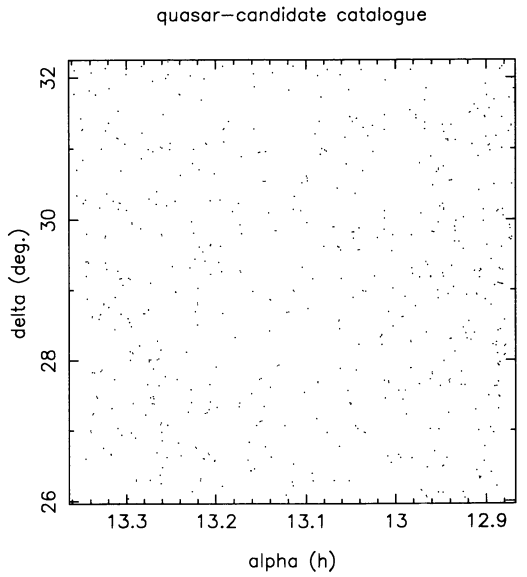

Fig. 10. Bidimensional distribution of the quasar candidates

5.2. *Identification*

We managed to identify the quasar candidates as already known UV–excess objects from three sources: B91, the Véron–Véron catalogue of quasars and active galactic nuclei (1993) and the white–dwarf catalogues of Luyten (1970, 1977, 1979). We of course eliminated from the candidate catalogue objects whose spectral nature has already been published; Table 6 shows the number of rejected objects of each identified type. The total number of these identified objects is 75, they are listed in Table 7 with column captions identical to those described in Sect. 6 (symbols defining the astrophysical nature of objects are those of B91).

Table 6. Object identifications

Type	number of objects
quasars already known	46
active galactic nuclei	4
white dwarfs	8
other stars	15
miscellaneous	2

Six known quasars (from the Véron–Véron catalogue) have been missed in our selection, we mean that six objects with a redshift lower than 2.2 and a V magnitude lying in our completeness range, i.e. brighter than 19.4, do not belong to our list of candidates. Namely: AH 1 (z=0.7, V=19.0), BG 57–5 (z=0.8, V=19.2), AH 25 (z=1.8, V=18.5), WEE 114 (z=0.5, V=18.00), US 383 (z=0.75, V=19.10) and 13h12+27°30 (z=2.1, V=18.80) (in this list, the names and redshifts of objects are from Véron–Véron, as well as photometry for the three first ones; V magnitude of WEE 114 is from B91 and that of the two last objects are from this work). The case of WEE 114 is well understood; this object (also named LB 32) is close to a 14th magnitude (presumed) star. Well separated in U, the one–threshold reduction technique of the PAPA procedure engulfed the companion in B and V. We note that, with the multi–threshold mode of our *pavés* procedure used in B91, this object was well separated and measured with $U-V=-0.55$. US 383 was probably missed because of photometric inaccuracies due to its faintness. The case of the four other missed quasars is less clear. AH 1, BG 57-5, AH 25 and 13h12+27°30 all are slitless spectroscopy quasar candidates obtained with a 158 nm/mm grism; two of these redshifts (that of AH 1 and BG 57-5) are unpublished. Low redshifts from slitless-spectroscopy (i.e. measured without the Lyα emission line) are known to be very dependant on the correctness of line identification. This added to the low accuracy of the published magnitudes and to the possible variablity of objects close to our cut–off make not clear that AH 1, BG 57-5 and AH 25 were lying in the redshift and magnitude ranges of our survey. At last, the colours we measure for 13h12+27°30 would be characteristic of a standard quasar at $z \simeq 2.5$.

5.3. *Proper motion*

In order to implement the proper–motion rejection criterion among the quasar candidates, we have paired together the Palomar V_{1962} and OCA V_{1990} plates. As some objects are expected to have moved in this span of 27.92 years, the maximum discrepancy between positions admitted for object cross–identifications has been set to 10.0 arcsec, and not only 2 arcsec as in Sect. 4.7. Therefore, misidentifications are here possible; we tried to avoid them by eliminating associations between objects showing atypical flux ratios. This is an efficient way to ensure the pairing but it may cause the loss of strongly variable objects. 12415 objects belonging to the 22–square–degree field common to both plates have been associated in that way; we have plotted in Fig. 11 the histogram of discrepancies between positions measured, for these objects, on the two different plates respectively.

As the estimated value of mean and standard deviation of the gaussian component of this histogram are respectively about 0.6 and 0.35 arcsec, we decided to eliminate quasar candidates showing position discrepancies larger than 2.0 arcsec; we believe that such discrepancies are due to a proper motion of the object, larger than about 0.07 arcsec per year (524 star–like objects among our sample show such a motion). This is not a so severe threshold but it is to note that our reduction chain is not presently aimed at being optimized for very accurate proper–motion measurements (see Soubiran 1992 for milliarcsecond proper–

Table 7. Objects already spectroscopically identified (see Sect. 6 for meaning of the notes)

No.	Identification	Alpha 2000	Delta 2000	U	B	V	Note
173349	LP 321-181 (WD)	12 52 16.99	+31 59 22.8	12.90	13.05	12.85	
174974	LB 11394 (QSO)	12 52 25.00	+29 13 21.2	16.80	17.65	17.45	BG B
173433	LB 7291 (Sy2)	12 52 28.05	+31 42 45.9	17.50	18.35	18.10	
175618	A2 120 (QSO)	12 52 42.54	+28 12 47.2	18.15	18.70	18.60	BG U
170351	LB 11408 (QSO)	12 53 17.70	+31 5 50.7	16.35	17.20	17.00	
170879	HZ 35 (sdB)	12 53 18.57	+30 6 30.1	14.50	15.80	16.15	
168386	SSII 229 (Ap)	12 54 3.66	+28 51 46.6	12.00	12.25	12.30	
158147	TN 673 (sdO)	12 56 4.94	+28 7 19.4	12.15	12.95	12.90	
157658	US 19 (QSO)	12 56 5.67	+28 49 42.1	18.55	19.15:	19.45	
158635	SSII 234 (A0)	12 56 23.79	+27 28 38.7	13.55	13.30	13.50	
154730	TN 140 (sdB)	12 56 27.50	+27 42 32.3	14.60	15.60	15.90	
149389	A2 221 (QSO)	12 56 53.28	+30 13 21.0	18.25	18.80	18.35	
141458	PB 3169 (QSO)	12 58 28.65	+29 12 21.0	18.20	19.15:	19.05	
138348	ZL 119 (QSO)	12 59 16.73	+27 53 46.1	18.15	18.65	18.60	
138642	HZ 38 (sdO)	12 59 21.35	+27 34 6.2	12.75	13.80	14.30	
138703	ST 285 (QSO)	12 59 23.39	+27 27 21.0	18.20		19.60	
138756	HZ 47 (sdOA)	12 59 26.10	+27 21 23.4	14.55	15.15	15.55	
138590	H4 1 (PNN)	12 59 27.81	+27 38 10.7	14.90	16.20	15.85	
134354	L 1408-19 (WD)	12 59 47.59	+27 34 1.4	14.75	15.45	15.45	
128601	A2 316 (QSO)	13 0 28.54	+28 30 10.3	17.10	17.55	17.30	
129678	(QSO)	13 0 41.44	+27 27 33.5	19.25:		19.30	
128724	A2 327 (QSO)	13 0 48.12	+28 23 20.7	16.75	17.85	17.90	
124334	A2 330 (QSO)	13 1 0.87	+28 19 44.7	16.65	17.65	17.40	
123463	A2 333 (WD)	13 1 8.21	+29 26 7.9	17.15	17.70	18.05	
124308	5C 4-127 (QSO)	13 1 20.14	+28 21 37.1	18.35		19.30	
118964	F 71 (B8III)	13 1 52.97	+29 34 57.5	10.55	10.50	10.70	NPM
117518	PB 3232 (AG)	13 1 54.79	+32 5 48.3	16.55	17.20	16.70	
116318	LB 27 (sdB)	13 2 41.78	+27 40 42.3	12.95	13.90	14.35	NPM
114425	PB 3252 (QSO)	13 2 41.82	+30 22 12.6	18.15	19.10:	18.90	
111704	TN 694 (QSO)	13 3 13.02	+28 11 7.5	16.50	17.50	17.35	NPM
108345	TN 143 (sdO)	13 3 46.67	+26 46 30.6	14.05	15.45	15.80	
105913	W 33211 (QSO)	13 3 53.64	+30 26 33.2	17.10	17.65	17.40	NPM
102796	US 211 (QSO)	13 4 9.60	+29 19 42.9	18.45	18.80:	18.95	
101691	PB 3276 (QSO)	13 4 16.35	+31 24 8.5	18.35	19.00:	18.80	
103569	HZ 39 (WD)	13 4 48.68	+28 7 29.6	14.05	15.20	15.60	NPM
94495	W 22722 (QSO)	13 5 54.73	+30 32 52.4	17.20	17.90	17.45	NPM
96871	PB 3297 (NHB)	13 5 59.71	+26 50 36.9	12.75	12.80	12.90	
90369	LB 30 (QSO)	13 6 16.67	+31 5 29.4	16.70	17.95	17.75	NPM
91093	PB 3310 (QSO)	13 6 26.23	+29 52 18.5	18.15	19.20:	18.85	
91423	AH 3 (QSO)	13 6 34.02	+29 24 43.5	18.95		19.50	
90501	US 272 (QSO)	13 6 34.25	+30 49 33.8	18.85	19.00:	19.00	NPM
87776	US 283 (QSO)	13 6 55.49	+29 4 33.9	18.45	19.20:	19.25	
87601	BG 57-9 (QSO)	13 7 2.70	+29 18 42.3	19.35:		19.80	
87818	PB 3324 (AG)	13 7 4.65	+29 1 32.4	18.35	18.80:	19.10	
87371	AH 9 (QSO)	13 7 22.44	+29 33 43.8	19.00		19.50	
83287	BG 57-18 (QSO)	13 7 45.88	+29 55 29.4	18.90	19.30:	18.90	
83525	US 303 (QSO)	13 7 49.35	+29 33 3.6	18.90		19.35	
84733	WEE 101 (QSO)	13 7 56.02	+28 3 23.8	18.85		19.10	
83337	PB 3336 (QSO)	13 8 4.02	+29 50 27.9	17.90	18.70	18.60	
79713	US 310 (QSO)	13 8 8.53	+29 34 49.2	19.10		19.30	
79912	PB 3340 (QSO)	13 8 16.10	+29 19 17.6	18.70	19.20:	19.35	
79427	W 23694 (QSO)	13 8 29.67	+30 5 39.3	16.50	17.05	16.75	NPM
77581	PB 3348 (QSO)	13 8 56.82	+27 8 11.7	17.80	18.55	18.45	
76398	PB 3349 (sd ?)	13 8 59.12	+29 5 58.5	18.20	18.65	18.45	
76304	KKC 64 (QSO)	13 9 11.88	+29 15 52.4	19.05		19.40	
71518	PB 3361 (WD)	13 9 56.31	+29 28 4.6	17.15	18.10	18.00	NPM
66989	US 367 (QSO)	13 10 23.24	+29 55 34.4	18.05	18.35	17.95	NPM
66788	US 369 (QSO)	13 10 24.61	+30 19 27.6	19.10:		19.65	
67973	WEE 116 (QSO)	13 10 36.13	+28 12 9.6	19.40:		20.15:	
63039	AH 28 (QSO)	13 11 4.26	+29 26 13.7	18.75		20.05:	
55437	WEE 122 (QSO)	13 12 9.90	+28 32 47.4	19.10:	19.20:	19.00	NPM
54445	PB 3389 (WD)	13 12 22.05	+30 16 6.8	17.80	18.45	17.85	NPM
54849	PB 3388 (AG)	13 12 22.11	+29 37 47.9	17.95	18.45	18.25	NPM
49443	TN 148 (em.)	13 12 56.29	+31 41 2.2	15.55	15.65	15.75	NPM
49636	HZ 42 (HBB)	13 13 13.33	+31 21 58.7	14.10	14.50	14.70	NPM
42357	PB3424+3425 (2WD)	13 14 21.75	+30 50 49.5	16.80	17.35	17.00	NPM
36998	(QSO)	13 15 42.57	+27 5 5.8	18.70		18.85	
33834	KUV 494-15 (NHB)	13 16 13.29	+31 56 52.9	14.70	14.40	14.75	
31523	HZ 43 (WD)	13 16 22.26	+29 5 59.2	11.45	12.80	12.55	
23107	PB 3471 (QSO)	13 17 37.86	+29 56 27.6	17.65	18.50	18.45	
21203	(QSO)	13 17 40.76	+26 58 5.1	19.10:	19.20:	19.20	
17128	US 542 (QSO)	13 18 19.10	+26 56 7.9	18.75	18.75	18.95	
11132	F 78 (A3)	13 19 42.97	+29 23 40.5	13.80	14.00	13.75	
8607	TN 153 (QSO)	13 19 56.15	+27 28 8.3	15.45	16.40	16.20	
8691	US 578 (QSO)	13 20 12.06	+27 14 47.4	18.20	19.10:	19.35	

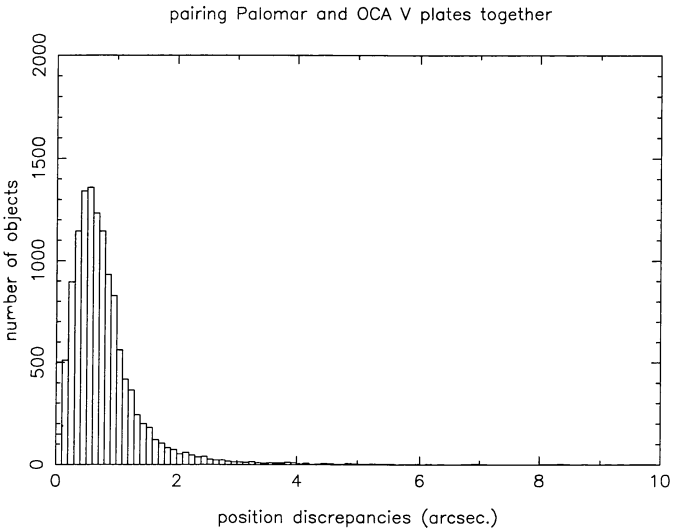

Fig. 11. Position discrepancies between 1962 and 1990 measurements (1 bin for 0.1 arcsec)

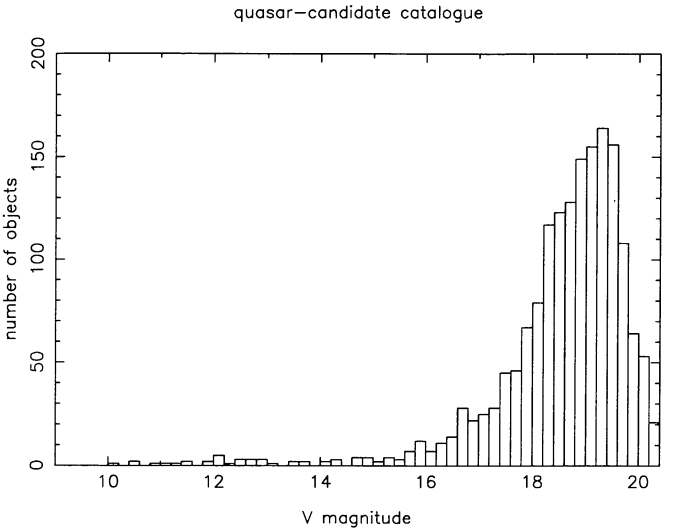

Fig. 12. V magnitude histogram of the quasar candidates (bin size is 0.2 mag.)

motion measurements with MAMA). Five candidates were rejected in that way. Two of them are white dwarfs already known: HZ 43 and A2 333 (we measure for them 0.21 and 0.11 arcsec/year as respective proper motions); the three others constitute good white–dwarf candidates, they are listed in Table 8 with celestial position for equinox 2000.0 at epoch 1990.25 (that of the OCA plate), photometry (magnitude are rounded by 0.05 steps, see Sect. 6 for meaning of colons), estimated proper motion μ and its direction angle θ (counted eastwards from the north, as usual). Note that three objects all have $U - B > -0.05$.

6. The catalogue of quasar candidates

After all these rejections, 1681 quasar candidates remained in the catalogue; the V-magnitude histogram of these objects has been plotted in Fig. 12. The brightest ones have the lowest a priori chance to be real quasars; this statement is reinforced by their absence in the Bright Quasar Survey (BQS) of Schmidt & Green (1983), even if 12% of the bright quasars may have been missed in the BQS (same reference). Taking into account the limiting magnitude ($B \simeq 16.2$) and photometric accuracy (0.27 in B and 0.24 in the selecting criterion $U - B < 0.44$) of the BQS, we consider as tentative quasar candidates those of our list that we measured with $B < 16$ and $U - B < -0.65$. We also note that the quality of the quasar candidates decreases close to our selection limit in $U - V$ and we consider therefore as marginal candidates objects having $0.0 < U - V < 0.1$.

The quasar–candidate catalogue is published in ASCII electronic form in the same format than Table 7. It is available free of cost via an anonymous ftp copy at the CDS — Centre de Données de Strasbourg, France — (ftp cdsarc.u–strasbg.fr or 130.79.128.5). Object positions range from $\alpha = 12$ h 52 min 08 s to $\alpha = 13$ h 21 min 33 s and from $\delta = +26°\ 02'$ to $\delta = +32°\ 13'$. As in Table 7, column captions are the following:

Column 1: detection number on the Palomar V plate
Column 2: name of object if known from B91
Column 3: right ascension (α) in hours, minutes, seconds for equinox 2000.0
Column 4: declination (δ) in degrees, arcminutes, arcsec for equinox 2000.0
Column 5: U magnitude (rounded by 0.05 steps); a colon indicates less certain values because lying within 0.5 mag. above the calibration limit
Column 6: B magnitude (rounded by 0.05 mag.) when available (some candidates have not been recovered on the B plate); idem for a colon
Column 7: V magnitude (rounded by 0.05 mag.); idem for a colon
Column 8: a note; label "NPM" for objects for which a proper motion could have been measured, if any greater than 0.07 arcsec/year (the other objects are too faint or outside the usable field of the OCA plate) and/or "BG" if the local sky background has been flagged in Sect. 4.3 for colours U, B and/or V. Moreover, the label NBQS (not in the BQS) is systematically assigned to objects with $B < 16$ and $U - B < -0.65$.

The Table 7 of spectroscopically identified objects and the list of white dwarfs candidates of Table 8 are also available in the same format at CDS since any statistical study has to deal with the concatenation of the three lists which is the only homogeneous data set.

Table 8. White–dwarf candidates

No.	α_{2000} (h min s)	δ_{2000} (° ′ ″)	V	$U-B$	$B-V$	μ (″/year)	θ (degrees)
55868	13 11 58.09	+27 54 21.1	19.00	−0.20:	0.25:	0.10	273
14207[1]	13 18 54.03	+30 55 36.3	13.45	−0.55	0.50	0.11	166
10920[2]	13 19 33.41	+29 42 04.3	18.50	?	?	0.07	134

[1] see Sect. 7
[2] missing on B plate, U−V = 0.10

7. Preliminary observation of candidates

The quasar candidates need to receive a spectroscopic confirmation. Their surface density is well suited to the use of a wide–field multi–object spectrograph at the focus of a 4–meter–class telescope. As a very crude (and only) preliminary test, three objects from the list of quasar candidates and one among our white–dwarf candidates have been observed (Vanderriest 1994) in one field of the MOS spectrograph at Canada–France–Hawaii 3.6m telescope.
— Object 18577, with $V = 19.60$ and $U - V = -0.20$:, is a quasar at $z = 1.48 \pm 0.02$.
— Object 18584, with $V = 19.05$ and $U - V = -0.05$, is a star (presumed from the halo).
— Object 18558 (also named PB 3487), with $V = 18.95$ and $U - V = -0.95$, is a quasar at $z = 0.61 \pm 0.02$.
— Object 14207, with $V = 13.45$ and $U - V = -0.05$ but that we rejected into Table 8 for its detected proper motion, is confirmed as a white dwarf.

If no statistics could of course be extracted from these cases, the known scarcity of quasars (and moving white dwarfs) among star–like objects seems to make these success ratios (2 among 3 and 1 among 1) significant to validate a minimal selection quality.

8. Conclusion and perspectives

We give a catalogue of 1681 low–redshift quasar candidates in a 40 square degrees area around the North Galactic Pole. Two by–products of the used method are also indicated, a general–interest multi–colour catalogue of all star–like objects in the field and a galaxy catalogue. We plan to extend this work to a total zone of 300 square degrees and to measure the quality and the completeness of the quasar–candidate selection by slit–spectroscopy of a subsample of star–like objects. We are also preparing the addition of photometric variability to our criteria (see e.g. Cristiani et al. 1990) with material acquired or to acquire with the OCA Schmidt telescope and a much deeper object catalogue with wide–band photographic material from OCA, using for example Technical Pan or IIIaF emulsions. We note moreover that the R colour available in addition of U, B and V for some 1962 Palomar fields of the zone could allow the selection of higher redshift quasar candidates. In the same time, we are using this growing homogeneous data set for a systematic search of highly scarcer objects like gravitational mirages or binary quasar candidates.

Acknowledgements. We would like to thank J. Berger who kindly made available to us the photographic plates he took at Palomar observatory and the OCA Schmidt team for the plate they have taken for us. Our gratitude is also due to J. Guibert and the whole MAMA scientific and technical team for the constant and efficient assistance we have received. In particular, J. Vétois provided his user–friendly image visualization software "VISUAL" and R. Chesnel was very efficient helping us for data handling. We also acknowledge the decisive contributions of C. Soubiran and C. Ducourant to the development of PAPA procedure. The massive reductions presented in this paper have been made easier by the effective computing facilities we benefit from in Liège; so, thanks to A. Detal, S. Elhoudriri and T. Wautelet, system managers. Discussions with E. Gosset were also fruitful. Object identifications have been made possible thanks to the meticulous work of A.-M. Fringant in B91. We are finally very grateful to C. Vanderriest for many helpful comments and for a first spectroscopy of four objects. This work was supported in part by contracts ARC 90/94-140 "Action de Recherche Concertée de la Communauté Française" and SC-005 "Services Fédéraux des Affaires Scientifiques, Techniques et Culturelles" (Belgium), HCM network CHRX-CT92-0044 (European Union) and by subsidies from the "GdR Cosmologie" (France).

References

Allen C.W. 1973, "Astrophysical Quantities" (3rd edition) (The Athlone Press, University of London) 200
Baum A. 1960, private communication to J. Berger and A.-M. Fringant
Berger J., Fringant A.-M. 1977, A&AS 28, 123
Berger J., Cordoni J.-P., Fringant A.-M. et al. 1991, A&AS 87, 389
Bijaoui A. 1980, A&A 84, 81
Cristiani S., Hawkins M., Iovino A., Pierre M., Shaver P. 1990, MNRAS 245, 493
Cristiani S., La Franca F., Andreani P. et al. 1991, "The Space Distribution of Quasars", ASP Conf. Series 21, 76
de Lapparent V., Geller M.J., Huchra J.P. 1988, ApJ 332, 44
Foltz C.B., Osmer P.S. 1988, Proc. of a Workshop on Optical Surveys for Quasars, eds. Osmer et al., p. 361
Goldschmidt C., Miller L., Mitchell P.S. et al. 1991, "The Space Distribution of Quasars", ASP Conf. Series 21, 93
Guibert J., Moreau O. 1991, The ESO Messenger 64, 69
Hancock S., Davies R.D., Lasenby A.N. et al. 1994, Nature 367, 333

Haro G., Luyten W.J. 1962, Bol. Obs. Tonantzintla y Tacubaya 22, 37
Hewett P.C., Foltz C.B. 1994, PASP 106, 113
Hoffleit D., Jaschek C. 1982, The Bright Star Catalogue (4th edition), Yale University Observatory
Irwin M., Mac Mahon R.G., Hazard C. 1991, "The Space Distribution of Quasars", ASP Conf. Series 21, 117
Kibblewhite E.J., Bridgeland M.T., Bunclark P.S., Irwin M.J. 1984, Proc. of the Astronomical Microdensitometry Conf., NASA Conf. Publ. 2317
Koo D.C., Kron R.G. 1982, A&A 105, 107
Luyten W.J. 1970, "White Dwarfs I", University of Minnesota, Minneapolis
Luyten W.J. 1977, "White Dwarfs II", University of Minnesota, Minneapolis
Luyten W.J. 1979, "The NLTT Catalogue", University of Minnesota, Minneapolis
Mac Gillivray H.T., Stobie R.S. 1984, Vistas Astron. 27, 433
Moreau O. 1992a, Proc. of the second DAEC Workshop "Distribution of Matter in the Universe", Observatoire de Paris–Meudon, p. 233
Moreau O. 1992b, thèse de doctorat, Université Paris 7
Pennington R.L., Humphreys R.M., Odewahn S.C., Zumach W.A., Stockwell E.B. 1992, Proc. of the conf. "Digitised Optical Sky Surveys", eds. Mac Gillivray and Thomson, 77
Purgathofer A.T. 1969, Lowell Observatory Bulletin 147, 98
Reboul H., Fringant A.-M., Vanderriest C. 1986, Proc. of IAU Symposium 119 "Quasars", eds. Swarup and Kapahi, p. 553
Reboul H. 1988, Proc. of the DAEC. Workshop "Large Scale Structures", Observatoire de Paris–Meudon, p. 53
Röser S., Bastian U. 1991, PPM Star Catalogue, Astronomisches Rechen Institut Heidelberg
Schmidt M., Green R.F. 1983, ApJ 269, 352
Slezak E., Bijaoui A., Mars G. 1988, A&A 201, 9
Smoot et al. 1992, ApJ 396, L1
Soubiran C. 1992, A&A 259, 394
Stobie R.S., Morgan D.H., Bhatia R.K., Kilkenny D., O'Donoghue D. 1987, Proc. of IAU Colloquium 95, eds. Philip et al., p. 493
Stobie R.S., Chen A., O'Donoghue D., Kilkenny D. 1992, "Variable Stars and Galaxies", ASP Conf. Series 30, 87
Surdej J., Refsdal S. 1992, Highlights Astron. 9, 3
Vanderriest C. 1994, private communication
Véron–Cetty M.-P., Véron P. 1993, "A Catalogue of Quasars and Active Nuclei" (6th edition), ESO Sci. Rep. 13
Warren S.J., Hewett P.C., Osmer P.S. 1991, ApJS 76, 23